The Sol-Gel Synthesis of Epitaxial Oriented Dense α-Quartz Thin Films

Second Master Research Project

Author: Joshua Levinsky Student number: S2372169

Supervisor: Prof. Dr. B. Noheda

Second assessor: Dr. G.R. Blake

Daily supervisor: Jordi Antoja Lleonart

Date: 19-07-2017

University of Groningen
Zernike Institute
for Advanced Materials

Table of Contents

1. INTRODUCTION

1.1 MOTIVATION AND QUARTZ BACKGROUND INFORMATION

The mineral quartz (SiO_2) has been known since prehistoric times and has seen practical use ever since.[1] Quartz is the second most abundant mineral found in the earth's crust after feldspar which explains its widespread use and interest in it still to this day. It consists of the most abundant elements found in the Earth's crust. (see figure 1)

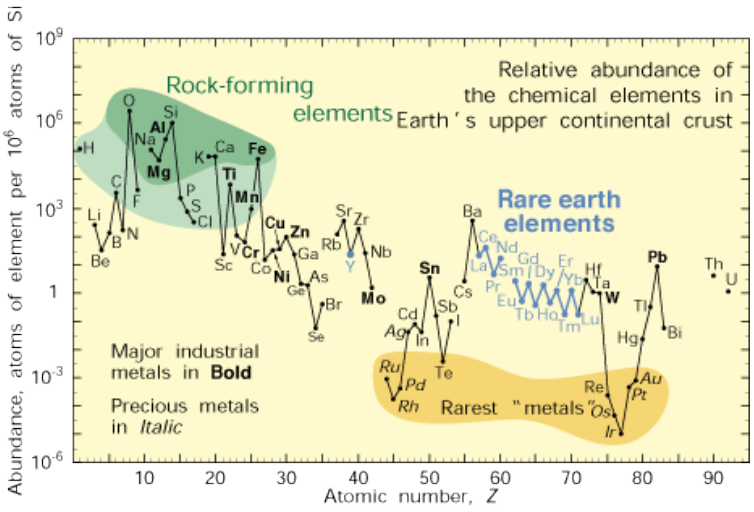

Figure 1 The relative abundance of the elements found in the Earth's crust is plotted against the atomic number Z. Taken from: https://pubs.usgs.gov/fs/2002/fs087-02/images/fig04.gif

The mechanical properties, most importantly its hardness, were utilized in the form of tools during the Stone Age.[1] The piezoelectric properties of α-quartz were discovered by the Curie brothers in 1880. [2] Quartz has a trigonal crystal structure with spacegroup $P3_221$ which does not contain an inversion center making it piezoelectric. Unlike many other piezoelectric materials α-quartz is not ferroelectric as it has no remnant polarization at zero electric field. The crystal structure of α-quartz can be seen in figure 2.

The piezoelectric properties were first exploited and implemented into an application in 1921 when the first quartz crystal oscillator was developed.[3] The quartz crystal oscillator is still being used to this day in some form or fashion. Where it was integrated into clocks in the past, it is integrated in microprocessors today. α-quartz has a high quality factor (Q), which means that it has a narrow frequency response. That property is beneficial for applications where precise frequencies are required.[4] With the increasing miniaturization of electronics, electronic parts made with quartz have to become smaller as well. The standard for producing high quality quartz crystals has been the hydrothermal synthesis method for a long time.[4,5]

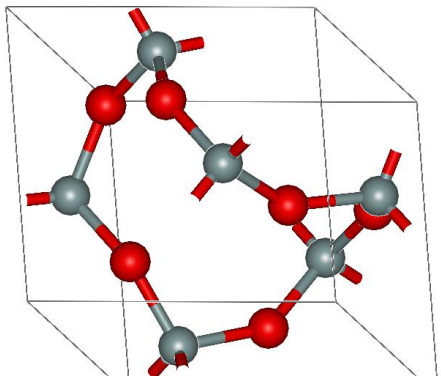

Figure 2 The crystal structure of α-quartz. Taken from: By Materialscientist - English Wikipedia, en:File:A-quartz.png, Public Domain, https://commons.wikimedia.org/w/index.php?curid=9838526

α-quartz crystals with the right dimensions for microelectronics cannot be synthesized directly using the hydrothermal method. Quartz crystals have to undergo extensive post processing involving micromachining to get them to the right dimensions.

Since the discovery of the piezoelectric properties of α-quartz there have been many materials found with better piezoelectric properties than α-quartz like the state of the art materials lead zirconium titanate (PZT) or barium titanate (BTO). Despite their better piezoelectric properties the state-of-the-art materials in general have two great disadvantages which α-quartz does not have. Quartz is made up of non-toxic elements, while for example PZT contains lead which can be very toxic to various life forms. This is an important aspect for future in vivo applications. The current power supply of implantable electronic devices, for example pacemakers, depends on batteries which have to be surgically replaced after they are depleted. These surgeries can be avoided by an implantable piezoelectric generator that could harvest the continuous energy output of for example a pulsating aorta, potentially powering a pacemaker indefinitely.[6,7] Also due to the abundant nature of quartz and other silica phases in the earth's crust, the production of α-quartz is not as expensive compared to the production of other piezoelectric materials which consist of elements which are scarcer and therefore more expensive. (see figure 1)

Considering that α-quartz is nothing more than crystallized silica, the ideal situation for synthesizing α-quartz thin films would involve direct crystallization of silica thin films. At this point in time the process of creating thin films of amorphous silica is well understood. The Stöber process developed in the 1960's[8] made it possible to precisely control the properties of silica nanoparticles which in turn could be used to make thin films of α-quartz with tunable properties. However crystallizing amorphous silica to quartz is not trivial.

The biggest problem for making thin films of α-quartz is to selectively grow α-quartz instead of the other silica polymorphs that are stable at room temperature. Looking at the phase diagram for silica (figure 3) it can be seen that α-quartz should be the only stable phase at room temperature. However cristobalite and tridymite phases are metastable at room temperature and are often formed instead of α-quartz. Only recently α-quartz nanoparticles have been synthesized by the crystallization of amorphous nanoparticles produced by the Stöber process.[4] The crystallization of silica was aided by depositing devitrifying agents, akali or akali earth metals, homogenously throughout the particles. The metal cations act as heterogeneous catalysts which lower the melting point of the silica and promote devitrification at lower temperatures. By tuning the catalyst used and the concentration of the catalyst, α-quartz could be selectively grown.

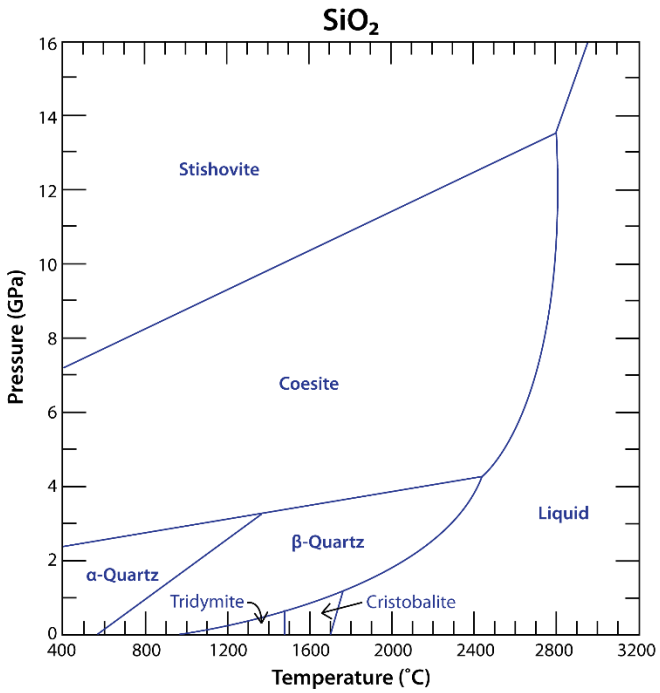

Figure 3 Phase diagram of SiO_2 Taken from: https://d32ogoqmya1dw8.cloudfront.net/images/NAGTWorkshops/mineralogy/mineral_physics/sio2_high_p.v6.png

Thin films of α-quartz have mainly been epitaxially grown on non-silicon substrates like sapphire (Al_2O_3) by thermal evaporation under ultrahigh vacuum or chemical vapor deposition.[9,10] Growing epitaxial thin films of α-quartz on silicon would be preferred due to the fact that silicon is the industry standard as a substrate for electronic components due its semiconducting nature and it also can be doped to improve its conductance which turns it into a back electrode. The group of Carretero-Genevrier has successfully selectively grown epitaxial oriented α-quartz thin films on silicon (100) by combining the Stöber process with dip coating. Their method, which will be explained further later in this report, uses surfactants that self-assemble to create meso- and macroporous amorphous silica films which depending on what surfactant and catalyst is used can lead to dense or porous crystalline films. The crystallographic direction of the Si (100) is cited as the main reason for the selective growth of α-quartz due to the close similarity of the lattice parameters,[4] however the choice and concentration of catalyst used also has a significant influence on what phase is formed, the degree of preferred orientation, the degree of crystallinity and the resulting microstructure. [5]

1.2 SOL-GEL CHEMISTRY

The Stöber process is a sol-gel synthesis method to create monodisperse silica nanoparticles. Developed in the 1960's[8] this method has become the standard for creating silica nanoparticles and has been modified over the years to create a whole range of different nanoparticles with controllable sizes, morphologies and added functional groups. The nanoparticles can be deposited on substrates yielding either aerogels, xerogels, dense films or individual nanoparticles depending on the deposition technique and processing parameters.

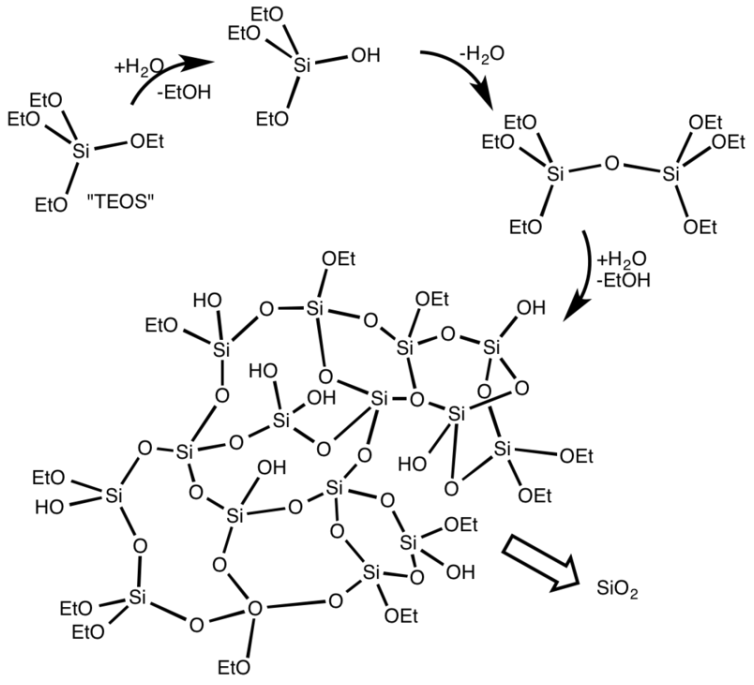

Figure 4 Schematic drawing of the hydrolysis and condensation reactions that lead to silica nanoparticles. Taken from: By Smokefoot - Own work, CC BY-SA 3.0, https://commons.wikimedia.org/w/index.php?curid=25698603

1.2.1 STANDARD STÖBER PROCESS

In the standard Stöber process first reported in 1968, silica nanoparticles are synthesized by adding tetraethylorthosilicate (TEOS) and ammonia (NH_3) to an alcoholic solvent (primarily methanol or ethanol). [8] The TEOS is hydrolyzed in the presence of NH_3 which acts as a base catalyst. This reaction produces ethanol and a mixture of different ethoxysilanols (from $Si(OEt_3)OH$ to $Si(OH)_4$). A condensation reaction can then occur between the ethoxysilanols themselves or between an ethoxysilanol and TEOS.[11] This reaction releases water and a dimer is formed. A schematic illustration of the condensation and hydrolysis reactions is shown in figure 4. The hydrolysis of TEOS can also be catalyzed by an acid (HCl), however the condensation rate between the silica species is lowered significantly when using an acid catalyst.[12,11] The condensation rate is plotted against the pH in figure 5. In this figure it can be seen that the isoelectric point (IEP) of the silica species is at pH ~2. This means that below

this pH the ratio between positively charged silica species and the neutral species is >1. At pH values above the IEP of the silica species the dominant silica species present in solution is negatively charged. The negatively charged species promote the nucleophilic attack step of condensation reaction which increases the condensation rate.[11]

The cycle of hydrolysis and condensation reactions then occurs until all the TEOS has reacted with itself. Due to the tetrafunctional nature of the TEOS, crosslinking occurs and polymers/aggregates are formed.[12] The size of the nanoparticles formed is dependent on the concentration and amount of ammonia, water and TEOS used[11]. Increasing the amount of water or ammonia leads to an increase in particle size due to an increase in pH and water available for the reaction, which increases the reaction rate of the condensation reaction.

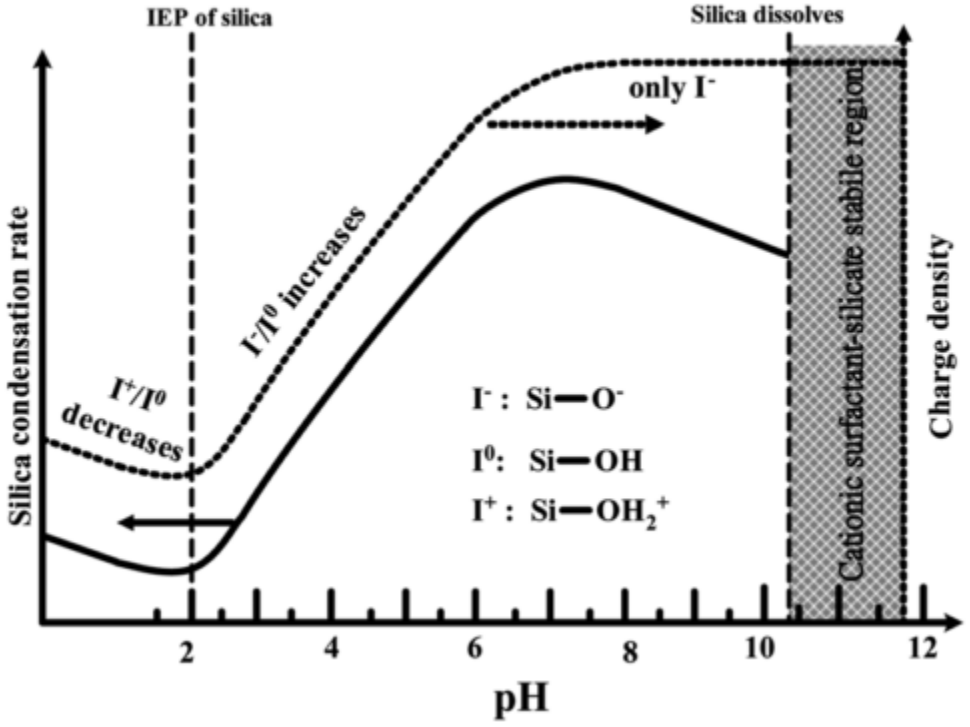

Figure 5 Condensation rate of silica is plotted against the pH and the charge density. Taken from ref 11.

The amount of TEOS used is inversely proportional to the particle size due to the increase of nucleation sites.[11]

1.2.2 MESOPOROUS SILICA NANOPARTICLES

Mesoporous silica nanoparticles are nanoparticles that have pores that are between 2 and 50 nm according to the IUPAC. These can synthesized using an altered version of the Stöber process. By the addition of surfactants (amphiphiles, either ionic or non-ionic) or block co-polymers to the reaction mixture used in the standard Stöber process, inverted micelles are

formed due to the polar nature of the silica species. These inverted micelles are then spread throughout the nanoparticles. After removing the solvent, the obtained nanoparticles are calcined above the combustion temperature of the surfactant to remove the surfactant. After the calcination step mesoporous nanoparticles are left. The size of the mesopores can be controlled by the selection of the surfactant used. The longer the hydrophobic tail is of the surfactant, the larger the mesopores are.

The morphology of the voids in the nanoparticles can also be tuned by choosing a surfactant with a more bulky hydrophilic head group. These parameters influence the self-assembly of the surfactants which can lead to the formation of bilayers and other morphologies. [13] This in turn affects the morphology of the voids left in the nanoparticles after removing the surfactant.

1.3 PROCEDURE OF CARRETERO-GENEVRIER ET AL

The procedures followed in this project are also modified Stöber processes designed to create either macroporous, mesoporous or dense thin films of amorphous silica by dip coating. The biggest differences compared to the procedure to synthesize mesoporous nanoparticles is that this procedure uses an acid catalyst for the hydrolysis reaction of the TEOS and more ethanol is used than is standard (also known as the high dilution method[11]). HCl is used instead of NH_3 which means this reaction happens at pH 1-2 instead of 7-8 in the case of NH_3. At this pH the condensation rate between the ethoxysilanols is slow enough for hardly any condensation reactions occur. In this pH range the consequence of the slow condensation rate is that TEOS is fully hydrolyzed and a lot of nucleation sites are formed but do not grow significantly.[14] This means that no precipitation occurs and the nanoclusters of condensed TEOS stay in the solution. The condensation reaction primarily happens during dip coating.
The amount of ethanol is increased significantly compared to a standard Stöber process procedure. This ensures that the concentration of the TEOS is lowered significantly meaning that the condensation rate is lowered and suppresses precipitation even further.[11]

1.3.1 MACROPOROUS AND MESOPOROUS FILMS

The mechanism of the formation of the macropores described in the procedure of Carretero-Genevrier et al,[4] involves the choice between ionic and non-ionic surfactants. The choice for cationic surfactants combined with the salts present in the solution results causes the adsorption of water from the atmosphere on the surface of the film. A $[S^+ A^- M^{x+}]$ complex between the cationic surfactant, the anion from the salt or acid and the metal cation is formed that stabilizes the water droplet.[5] This process can be seen in figure 6. Non-ionic surfactants like Brij-56 or poly(butadiene-ethylene oxide) (PB-PEO) cannot form this complex and therefore the water droplets do not form on the film leaving only a mesoporous film.

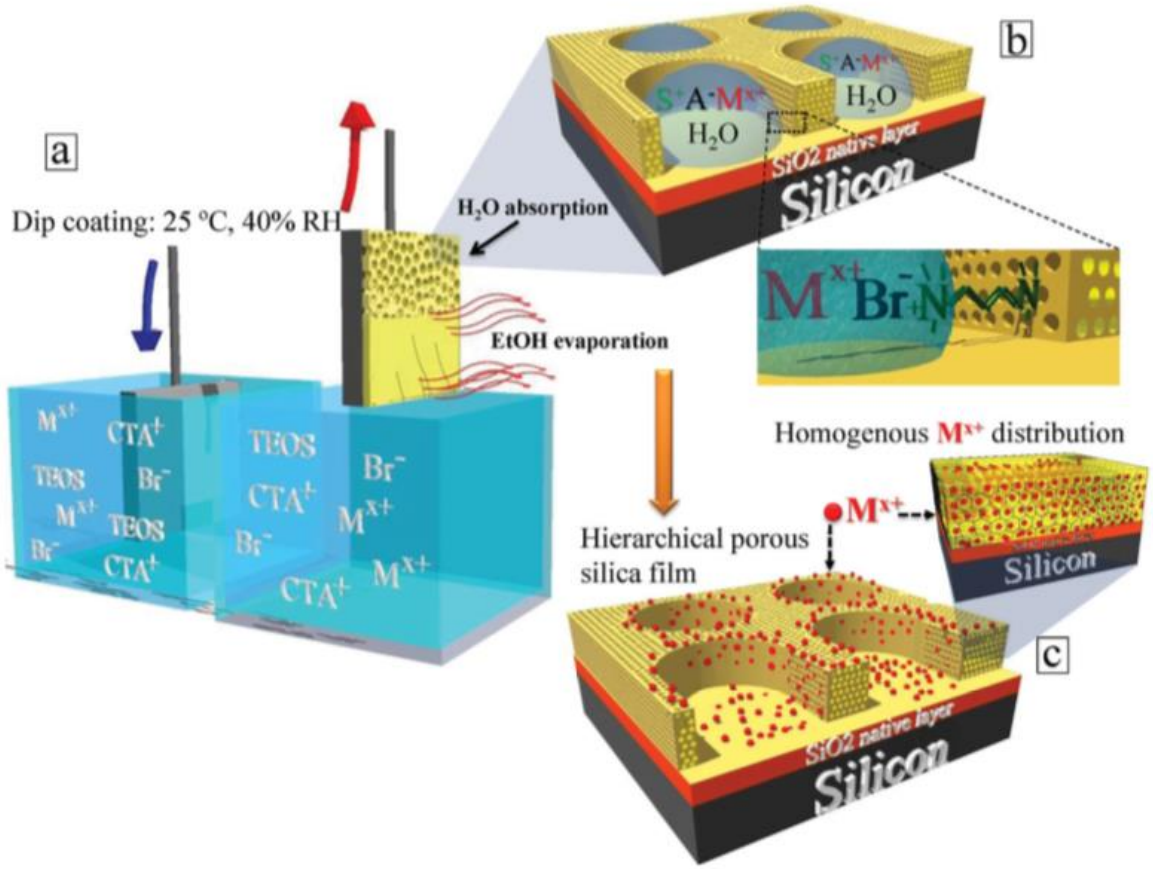

Figure 6 Image schematically showing the steps that occur on the film after dip coating producing hierarchical porous silica films. Taken from ref 5.

1.3.2 DENSE FILMS

To create dense quartz films the method for mesoporous films is used. The use of non-ionic surfactants leads to the formation of mesopores instead of macropores, due to the suppression of the adsorption of water from the atmosphere. The size of the mesopores formed can be controlled by the size of the hydrophobic tail of the non-ionic surfactant used. In the procedure of Carretero-Genevrier[15] a diblock copolymer PB-PEO is used to create 40 nm pores, while the use of the surfactant Brij-56 leads to formation of 3.5 nm pores.[4] The size of the pores has a significant effect on the eventual microstructure of the film after the thermally activated crystallization step that is performed at 1000˚C. The 3.5 nm pores of the film produced with Brij-56 collapse when exposed to this temperature resulting in a dense film. The 40 nm pores of the PB-PEO film can withstand these temperatures and produce a mesoporous film.

1.4 CRYSTALLIZATION OF α-QUARTZ

The homogenous distribution of the salt throughout the mesoporous film made with Brij-56 is the most important aspect of the procedure from the article by Carretero-Genevrier et al,. The alkali or alkali earth metal cations present throughout the film act as heterogenous catalysts which lower the melting temperature significantly. The material can then crystallize by slowly cooling down. The crystallization reportedly occurs at the interface between the quartz and the silicon substrate. The precise mechanism of the heterogenous catalysis is still under debate, however the crux of the proposed mechanisms is the disruption of Si-O tetrahedra by breaking some of these bonds. This induces defects in the amorphous silica network and therefore lowers it melting point.[16]

Silica has been crystallized using different methods as well. The crystallization of silica has also been induced on a glass substrate by placing a NaCl crystal on the surface.[17] Silica nanoparticles have also been crystallized using a modified Stöber process procedure where another metal alkoxide, for example titanium tetrabutoxide, is added alongside TEOS.[18] In this approach the melting agents are integrated in the amorphous silica matrix by participating in condensation reactions with the TEOS that is present in solution. Due to the mixing of reactants on a molecular scale a higher degree of homogenously distributed metal cations is ensured than in the procedure described by Carretero-Genevrier. These other methods to crystallize silica have also been used in this project. The experimental methods are presented in another section of the report.

1.5 DIP COATING AND EVAPORATION INDUCED SELF-ASSEMBLY

In the procedure described by Carretero-Genevrier et al, the thin films are made by dip coating Si (100) wafers into the reaction mixture containing the fully hydrolyzed TEOS, surfactants, alkali or alkali earth metals, water and ethanol. In the reaction mixture the concentration of the surfactant is below the critical micelle concentration (CMC) which is the concentration at which micelles begin to form in solution. This is due to the excess amount of ethanol present in the reaction mixture compared to the standard procedure to synthesize mesoporous nanoparticles.

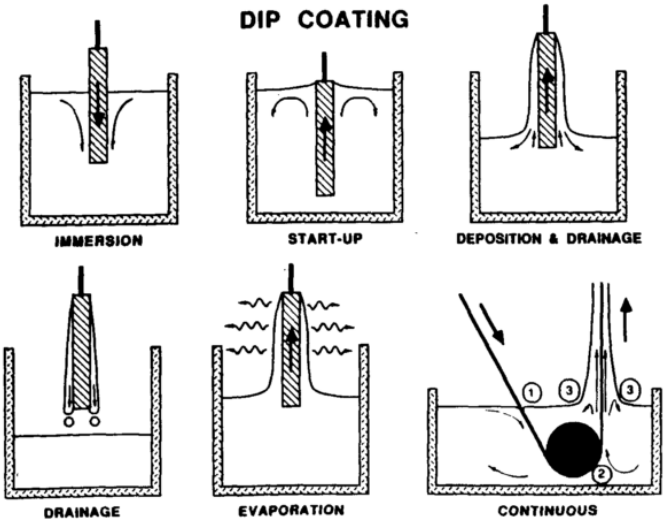

Figure 7 Schematic images of the five stages of dip coating single wafers and one image showing the continous method of dip coating. Taken from ref 19.

The formation of micelles which lead to the mesoporous nature of the films happens during dip coating. Dip coating is a deposition technique which produces thin films of a desired coating of a liquid or gel on a solid substrate. The batch dip coating process can be divided in five stages; immersion, start-up, deposition, drainage and evaporation.[19] (see figure 7) The most important steps for creating thin films of silica is the deposition and evaporation step. During the deposition, evaporation of ethanol, HCl and water occurs. This means that the concentration of the surfactant is increased above the critical micelle concentration and through self-assembly inverted micelles are formed throughout the deposited film.[14] At this stage condensation reactions between the hydrolyzed TEOS will also start to occur more significantly producing a thin film of amorphous silica. These steps are illustrated in figure 8. The metal cations present in the solution will be kinetically trapped within the surfactant-silica mesophase due to the fast evaporation kinetics.[4] This ensures a homogenous distribution of the salts throughout the film, which is essential for obtaining a high degree of crystallinity of the thin film in the end. To ensure the production of homogenous thin films the substrate should also be fully wetted. To promote the wetting of the silicon substrates, they are exposed to an UV/ozone lamp prior to dip coating to oxidize the surface, which ensures full wetting of the substrate by the polar silica species in the reaction mixture.

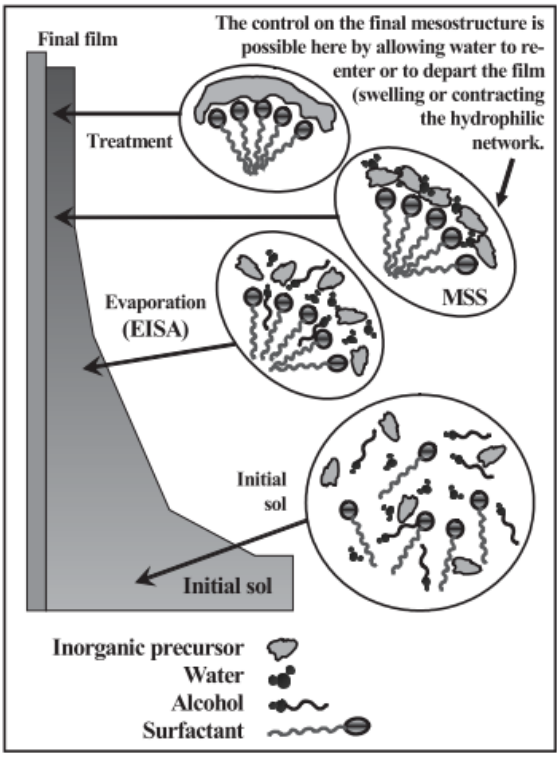

Figure 8 Image schematically showing the evaproation induced self-assembly of the surfactants during dip coating. Taken from ref 14.

1.6 PROJECT OULINE

In this project attempts were made to synthesize epitaxial oriented dense thin films of α-quartz on Si(100) by wet chemical synthesis methods based on a variety of reported procedures. Emphasis was put on the effect of the choice of salt on the crystallization of the different sources of amorphous silica as well as the homogenous distribution of the salt throughout the silica networks. Mesoporous silica films were made with altered versions of the procedures described by Carretero-Genevrier which influence the distribution of different salts throughout the film. Amorphous silica films were also made with Ti atoms integrated in the silica matrix instead of depositing the salt into mesopores. These films were annealed at 1000˚C to induce crystallization of the films. Attempts were also made to crystallize the native SiO_2 layer of the substrate by dip coating the substrate into a water

solution with different salts and annealing them at 1100˚C. Thin film X-ray diffraction was used to characterize the films. 2theta/omega scans were performed to identify the crystal phases that formed on the substrate. Reflectivity measurements were performed on the samples to determine the film's thickness. AFM measurements in tapping mode were performed to image the microstructure and surface of the annealed films. Specific features of crystallites can also be imaged in these measurements. The SEM was used to image the surface using secondary and backscattered electrons. EDS measurements were performed using the EDAX detector to gain an insight on the elemental composition of the films an particles found on the films.

The research question of this project comes down to:
What are the essential parameters, when using sol-gel chemistry methods combined with dip coating, to ensure homogenous thin films of oriented α-quartz and what are the effects of different salts on this process?

2. EXPERIMENTAL METHODS

2.1 THIN FILM XRD

Thin film X-ray diffraction is a characterization technique which can provide information on the crystal phases present on a thin film sample, their respective orientations as well as the thickness of the deposited film. The theoretical basis for this technique is the same for all X-ray diffraction techniques. When a crystal is irradiated by X-rays only the planes that are in the diffracting condition, dictated by Bragg's law (eq 1.), diffract with constructive interference and produce a signal that can be detected.

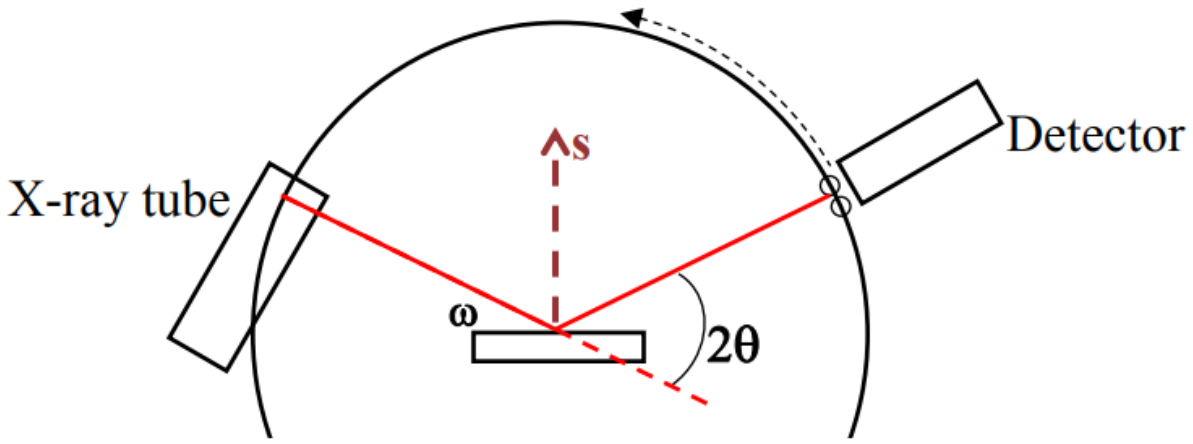

Figure 9 Schematic representation of the TFXRD setup in Bragg-Brentano geometry. Taken from ref 20

$$n\lambda = 2d \sin\theta$$

(Bragg's law eq 1.)

2theta/omega scans were used to identify the crystal phases present on the samples. In this measurement the coupling between 2θ and ω keeps the measurement setup in the proper Bragg-Brentano geometry meaning that in this way the Bragg diffraction angles of the crystal planes that lie parallel to the surface of the sample can be measured.[20] This is known as standard out-of-plane diffraction.

Rocking curve measurements were also performed during this project. Rocking curve measurements provide information of the degree of orientation of a particular crystal phase. During this measurement a fixed 2θ value is selected at which there is a Bragg diffraction peak while the value of ω is varied continuously.[20] As a result the degree of orientation can be determined by looking at the FWHM of the acquired peak. The broader the peak, the less oriented that plane is. This only provides information about the orientation out-of-plane.

Pole figure measurements were also performed during this project. In this measurement a single fixed 2θ value is taken at which a Bragg diffraction peak is located. During the measurement phi (rotation of the sample about the azimuthal axis without changing the angle between the sample and detector) and chi values are varied continuously providing additional information about the orientation of the crystals present on the sample. Also additional peaks belonging to other phases or planes can be found during this measurement that are in the diffraction condition at certain phi and chi angles. This therefore also provides information about the in-plane orientation of the crystals.

The instruments used in this project are the Philips X'pert and Panalytical X'Pert PRO MRD four axes thin film diffractometers using copper X-ray sources with wavelength λ=1.540598 Å in combination with a monochromator. The detector used in the setup of the Panalytical X'Pert PRO MRD is a PIXcel 3D detector which can measure 255x255 pixels in the 2θ and its perpendicular direction. This means that 255 2θ values are measured simultaneously, significantly speeding up measurements. 2theta/omega scans were performed using a 2θ range from 10-45˚. The data from the 2theta/omega scans were analyzed by plotting the data and then assigning peaks to crystal phases by comparing the peaks to calculated X-ray diffraction patterns generated from known crystallographic .cif files. The pole figures were analyzed and plotted using a software package from Panalytical called Data Viewer.

2.2 AFM

Atomic force microscopy (AFM) is a characterization technique that can probe the surface of conducting or insulating samples and image them. In the standard setup of this technique there is a cantilever which moves across the surface of a sample, while there is a laser that reflects off the cantilever onto a photosensitive detector. This monitors the height or bending of the cantilever while it moves across the surface and performs a line scan.[21] There are two main modes for AFM; contact and tapping mode. Considering only tapping mode is used in this project, contact mode will be left out of consideration.

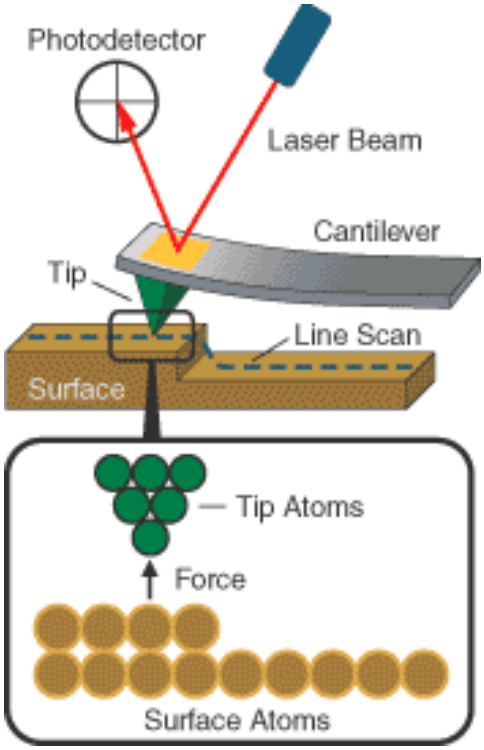

Figure 10 Schematic representation of a standard AFM setup. Taken from: http://www.keysight.com/upload/cmc_upload/ck/zz-other/images/AFM_schematic.gif

To reduce the effect of interacting forces, like electrostatic interactions, friction and adhesion between the tip and the surface, on the deflection of the cantilever and the interpretation of the image, tapping mode is used. In this mode the cantilever does not touch the surface continuously as in contact mode but oscillates consistently above the sample and taps the surface on every downward swing. In tapping mode the amplitude of the oscillation of the cantilever is kept constant. When an interaction between the tip and the surface occurs the oscillation amplitude changes. To keep the oscillation amplitude of the cantilever constant the distance between the tip and sample is changed continuously. The magnitude of the effect of the interaction caused by "tapping" the sample on the oscillation amplitude is height dependent so this is used to create topography images.

The images were processed and analyzed using the Gwyddion software package.

2.3 CHEMICAL PROCEDURES

In this project most of the work that was done focused on the procedure described by Carretero-Genevrier et al,[15] to synthesize epitaxial oriented thin films of α-quartz. The procedures that were followed from paper in question describe the synthesis of macroporous and dense α-quartz films. Different versions of the procedure were used based on another publication by Carretero-Genevrier et al, and after consulting with Carretero-Genevrier himself.[22]

2.3.1 DENSE FILM PROCEDURE 1 (two pot synthesis)

A solution composed of TEOS:Brij-C10:H_2O:EtOH:HCl in a molar ratio of 1:0.05:5:25:0.7 was made in a 40 mL sealable glass vial. 3.4 g TEOS (16.3 mmol) was dissolved in a solution containing 24 mL EtOH (410 mmol), 0.95 mL HCl (37%) and 0.87 mL H_2O. 0.557 g of Brij-C10 is then added to the reaction mixture. A second solution containing 1 M $Sr(NO_3)_2$ is made with $Sr(NO_3)_2 \cdot 4H_2O$ and DI water. The p-doped silicon substrate is oxidized for 10 min under a UV/ozone lamp. The solution is stirred for a minimum of 2 h before dip coating an oxidized silicon wafer at room temperature with a withdrawal speed of 1 mm/s at a relative humidity <40%. Immediately after dip coating the samples are thermally treated at 450˚C on a hotplate with a sapphire support. Once the amorphous silica film is produced the film is dip coated in a 1 M $Sr(NO_3)_2$ solution. The films are then annealed at 1000˚C for 5 h under oxygen flow (12L/hour) with a ramp of 3C/min (5½ h) and slowly cooled down to obtain dense quartz films.

2.3.2 DENSE FILM PROCEDURE 2 (one pot synthesis)

The following procedure is an altered version of the procedure used to make macroporous films.

A solution composed of TEOS:Brij-C10:H2O:EtOH:HCl:$Sr(NO_3)_2$ in a molar ratio of 1:0.05:5:25:0.7:0.062 was made in a 40 mL sealable glass vial. 3.4 g TEOS (16.3 mmol) was dissolved in a solution containing 24 mL EtOH (410 mmol), 0.95 mL HCl (37%) and 0.87 mL H_2O. 0.557 g of Brij-C10 is then added to the reaction mixture. The p-doped silicon substrate is oxidized for 10 min under a UV/ozone lamp. The solution is stirred for a minimum of 2 h before adding 1 mL $Sr(NO_3)_2$ solution to the mixture just before dip coating an oxidized silicon wafer at room temperature with a withdrawal speed of 1 mm/s at a relative humidity of 40%. The films are then annealed at 1000˚C for 5 h under oxygen flow (12L/hour) with a ramp of 3˚C/min (5½ h) and slowly cooled down to obtain dense quartz films.

2.3.3 DENSE FILM PROCEDURE 3 AND 4

These procedures are altered versions of DFP 1 and 2. In this procedure the order of adding the chemicals to the reaction mixture is reversed. The surfactant Brij-C10 is first dissolved in EtOH and HCl without extra water and afterwards the TEOS is added drop wise to the solution. This solution is then left to stir overnight. In the two pot synthesis method (DFP 3) amorphous silica films are first made and are dip coated in a 1 M $SrCl_2$ solution afterwards with a calcination step at 450˚C in between. In the one pot synthesis technique (DFP 4) 1 mL of the 1 M $SrCl_2$ solution is added to the TEOS reaction mixture and stirred for 10 min before dip coating.

2.3.4 DENSE FILM PROCEDURE 5 (one pot synthesis)

This procedure is based on the article published in JOVE by Carretero-Genevrier et al,.[22] The basis for this procedure is the same as DFP 4. In this procedure however the amount of HCl added to the solution is 1.5 mL instead of 0.95 mL. Also silicon substrates of 2x5 cm are used for dip coating.

2.3.5 DENSE FILM PROCEDURE 6 (Okabayashi + Carretero-Genevrier)

This procedure uses DFP 5 as a basis combined with a procedure described by Okabayashi et al,[18] where crystalline mesoporous silica nanoparticles are synthesized by the addition of titanium tetrabutoxide which is integrated into the silica matrix by participating in condensation reactions during dip coating.

In this procedure 0.4 mmol (0.14 mL) titanium tetrabutoxide and 0.04 g $CaCl_2$ is added to the reaction mixture of DFP 5 and is mixed overnight. One film was annealed after dip coating in the reaction mixture, two other films after being dip coated in the reaction mixture were dipped in 1 M $SrCl_2$ and $LiNO_3$ solutions before annealing.

2.3.6 DENSE FILM PROCEDURE 7 (Native oxide + salt)

Silicon substrates were oxidized for 10 min under a UV/ozone lamp and subsequently dip coated in either a ~2-3 M $SrCl_2$ solution, 5 M LiCl solution or 5 M NaCl solution. These samples were annealed at 1100˚C for 5 h with a ramp of 3˚C/min under an oxygen flow of 12L/h and were slowly left to cool down.

3. RESULTS AND DISCUSSION

3.1 DENSE FILM PROCEDURE 1

Three films were made with 1 M solutions of either $Sr(NO_3)_2$, $Ca(NO_3)_2$ or barium acetate. These three salts all reportedly produce oriented α-quartz films at this concentration.[5] The films dipped in either $Sr(NO_3)_2$ or $Ca(NO_3)_2$ produced films which showed no pore formation as expected but also seemed amorphous. The reported 3.5 nm pores[4] could also not be seen by the AFM measurement.

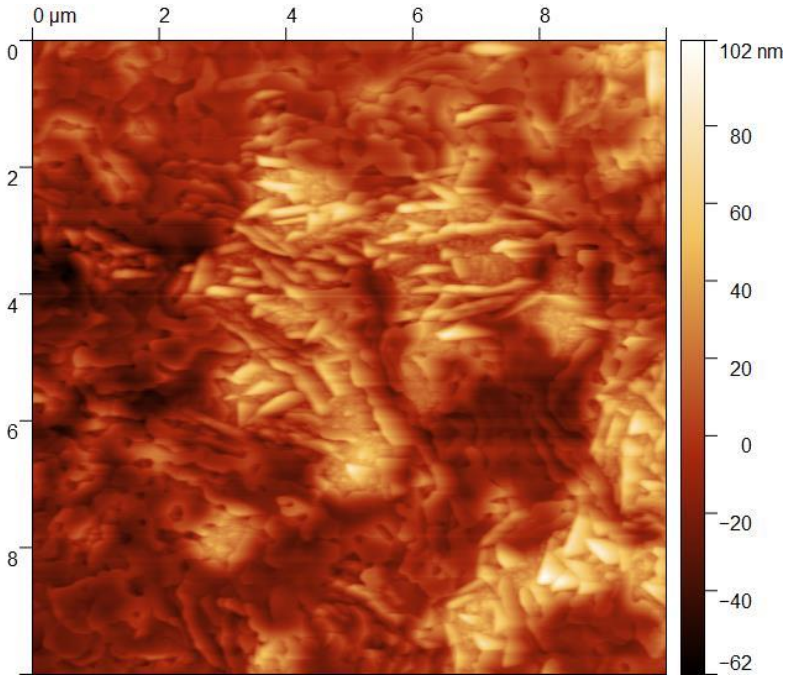

Figure 11 10x10 µm AFM image of the film dipped in barium acetate showing interesting features.

The film produced with 1M barium acetate solution still had a droplet of the solution on the surface when it went into the furnace. After annealing on the position where the droplet had been an opaque reflective spot was left. The AFM measurement showed that in the vicinity of this droplet interesting features could be seen. (figure 11) The irregular shapes seen on the rough surface look similar to AFM images of crystallites found on dense α-quartz films produced by Carretero-Genevrier. [4]

2theta/omega scans were performed on the samples to identify which crystal phases had formed. In the case of all the films no peaks were seen except for a multiple diffraction peak of the Si substrate at 33 degrees. Reflectivity measurements were also not conclusive on all samples. No fringes were seen in these measurements so the thickness of the films is unknown. The thickness of the samples could not be determined by either the roughness of the film or due to the small difference between the density of the Si substrate and the silica layer on top. No crystal phases could be identified presumably to the amorphous nature of the film in the case of the Sr and Ca dipped films or the low degree of crystallinity of the sample produced with Ba.

Attempts were made to remove the opaque spot left by the droplet by washing with water, HCl and HNO_3. None of these attempts were successful, so the spot was ruled out to be barium acetate but could still be a crystalline barium silicate phase or amorphous in nature.

In the paper by Carretero-Genvrier et al, (2013)[4] the synthesis of oriented α-quartz films is performed they show that in the case of $Sr(NO_3)_2$ only a fixed concentration of 1M produces oriented films while films made with $Ca(NO_3)_2$ have a larger concentration range at which they produce oriented α-quartz films. Therefore an emphasis was put on making dense α-quartz films using $Ca(NO_3)_2$ in the subsequent batch of films made.

Using DFP 1, 2 samples were made by dip coating the obtained amorphous silica film in 1 M $Ca(NO_3)_2$ solutions and one sample was manually dipped in the salt solution leaving a droplet on the surface of the film on purpose. AFM images, shown in figure 12, of the samples after annealing showed that the dip coated films looked amorphous with 40 nm voids spread across the surface. However these irregularly shaped voids do not show the same morphology expected from pore formation due to surfactant used.

In the case of the manually dipped sample with a droplet on the surface again interesting features were seen in the vicinity of where the droplet was before annealing. In this case hexagonally shaped "holes" were seen with a raised edge as well as lines towards the center of the "hole". The inside of the "hole" was scanned and oriented trapezoidal shapes could be seen. These images are shown in figures 13 and 14. These shapes look very similar to AFM images of quartz crystallites found on dense quartz films produced by Carretero-Genevrier.[4] These shapes could also be caused by a tip effect. These hexagonal shapes can therefore be assumed to be

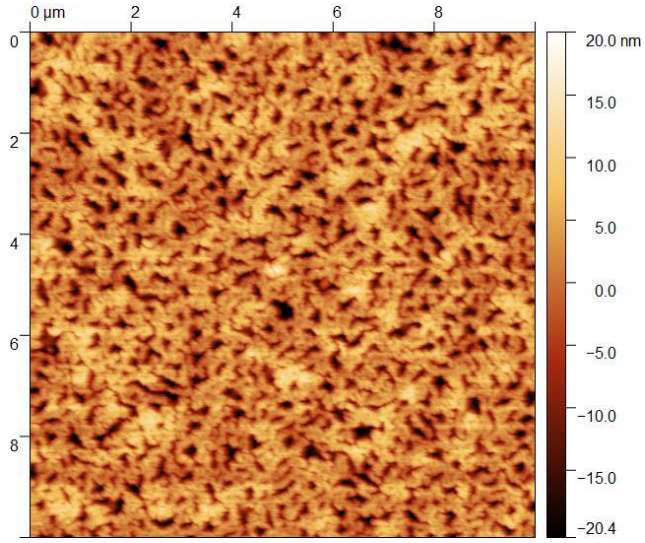

Figure 12 10x10 µm AFM image of an amorphous film that was dip coated in $Ca(NO_3)_2$.

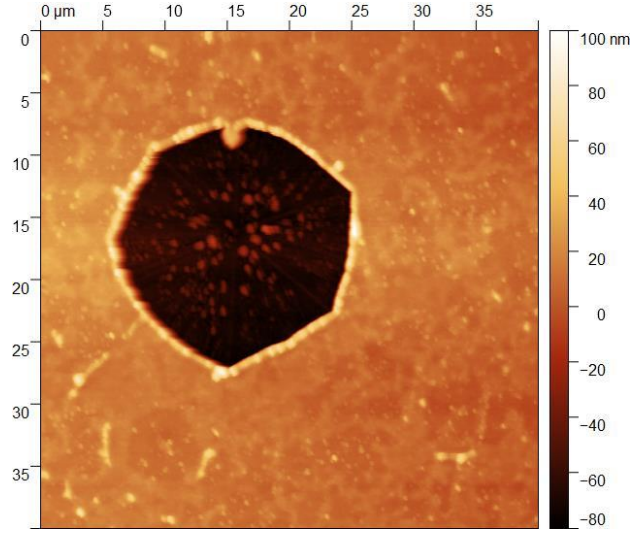

Figure 13 40x40 µm AFM image of hexagonal crystals found on films dipped in $Ca(NO_3)_2$

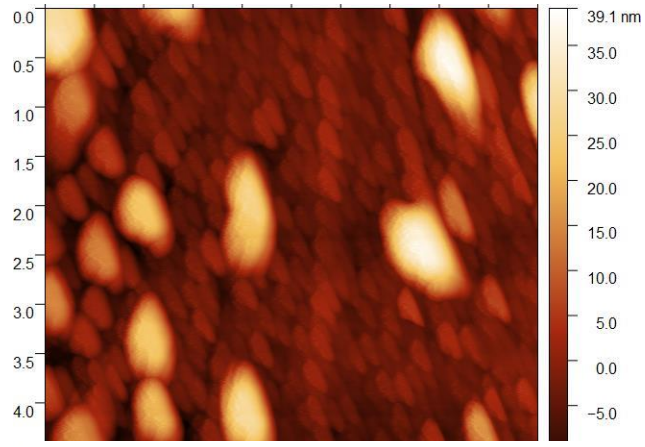

Figure 14 5x5 µm AFM image of oriented crystallites found on the inside of the hexagonal crystals

crystals. Only a handful of these hexagonal crystals could be seen on the surface.

2theta/omega scans were performed on the samples to identify which crystal phases had formed. In the case of all the films no peaks were seen except for a multiple diffraction peak of the Si substrate at 33 degrees. Reflectivity measurements were also not conclusive on all samples. No fringes were seen in these measurements so the thickness of the films is unknown.

It appears that only in the vicinity of the droplets of salt solution, crystallites of an unknown phase are formed. This could indicate that the distribution of the salt throughout the sample is not homogenous or that no salt is deposited in the mesopores of the amorphous silica film before annealing.

3.2 DENSE FILM PROCEDURE 2

Due to the fact that the salts are already present in the solution when the mesopores are formed it is assumed that the one pot synthesis method ensures a more homogenous distribution of the salt throughout the amorphous silica matrix.
Three films prepared with either 1 mL, 2mL or 3mL 1M $Ca(NO_3)_2$ solution added to the reaction mixture containing TEOS before dip coating.

After annealing AFM measurements showed that the surface of the sample dipped with 1 mL and 2 mL 1M $Ca(NO_3)_2$ solution was very similar.

The same oriented crystallite features can be seen in these images that were seen in the vicinity of the droplet of salt solution of the previous batch. Images were taken from two different positions on the film showing a difference in the degree of porosity across the film. The cause for this effect is unknown. The paper of Carretero-Genevrier describes that the use of non-ionic surfactants should not lead to the formation of macropores in general. [5] However an explanation for the emergence of pores can be found in the pH at which the hydrolysis reaction of the TEOS in solution is performed. At pH 1-2 it is not unlikely that the Brij-C10 is actually protonated and therefore is positively charged. At that point there is no difference in using a non-ionic or ionic surfactant and therefore macropores can be formed. It could also be that the relative humidity at which dip coating is performed is too high and water is still adsorbed significantly by the polar surface causing pore formation.

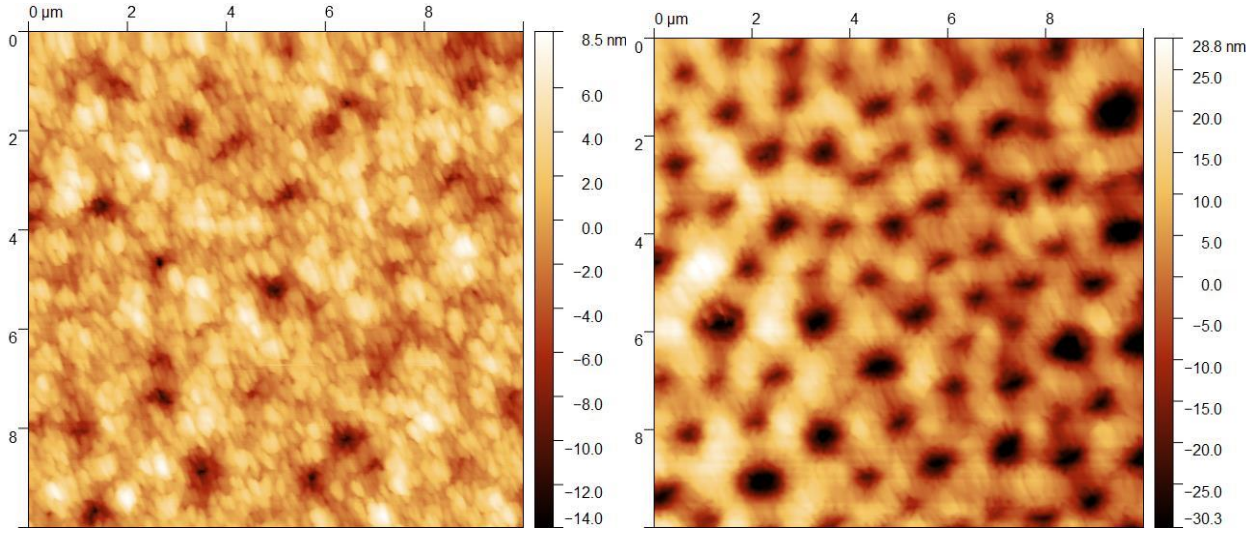

Figure 15 10x10µm AFM images of the same film at two different postions showing a difference in degree of porosity. The same oriented crystallites can be seen at both positions.

The sample made with 3 mL 1M $Ca(NO_3)_2$ solution showed different behavior. The AFM images only show very large particles on the surface of unknown origin. During the evaporation step of dip coating, water droplets could also be seen forming on the surface of the films. This is an indication that the salt concentration that was used is too high.

SEM images showed that on the sample made with 3 mL 1M $Ca(NO_3)_2$ solution does contain pores. Images made with backscattered electrons show the difference in elements on the surface. Lighter elements appear dark and heavy elements appear light. Around and in the pores light colored particles could be seen. (figure 16) This is also seen in the paper of Carretero-Genevrier et al, where they conclude they are $SrCO_3$ nanoparticles formed by the expulsion of the salt ions from the silica lattice which react with CO_2 and O_2 during annealing.[5] EDS measurements confirmed that the nanoparticles consist of Ca. Carbon is too light of an element to accurately measure with EDS so it is not confirmed that these are $CaCO_3$ nanoparticles. This indicates that the one pot synthesis method does provide a homogenous distribution of metal cations throughout the silica matrix.

2theta/omega scans were performed on two samples to identify which crystal phases had formed. In the case of the two films no peaks were seen except for a multiple diffraction peak of the Si substrate at 33 degrees. Reflectivity measurements were also not conclusive on the samples. No fringes were seen in these measurements so the thickness of the films is unknown.

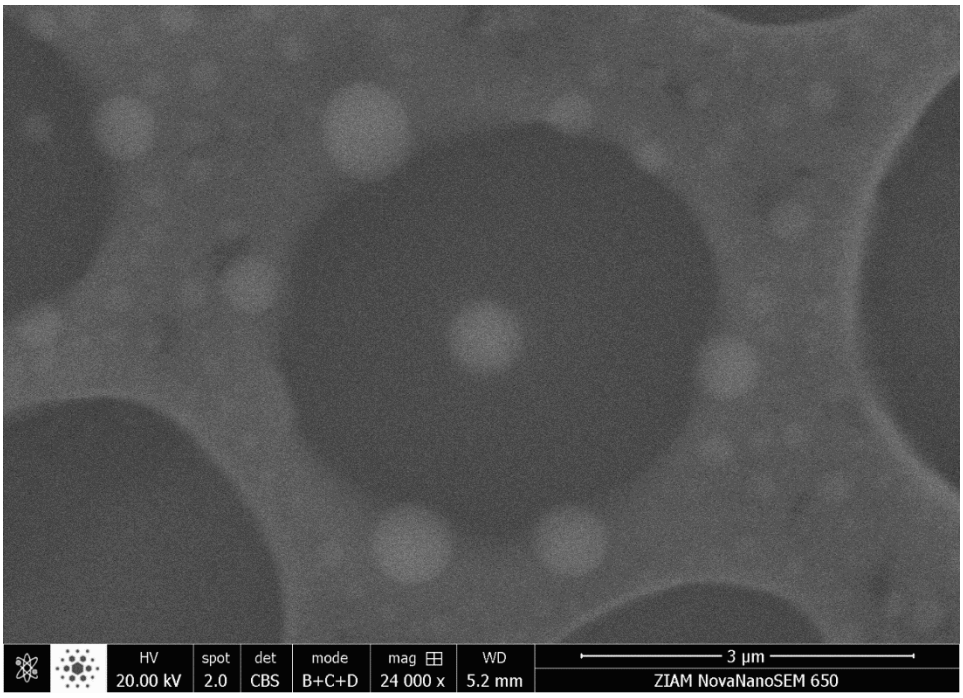

Figure 16 SEM image using BSE to image the nanoparticles containing Ca in and around the pores

3.3 DENSE FILM PROCEDURE 3 & 4

Two identical samples were made using DFP 3 and two identical samples were made with DFP 4. According to Carretero-Genevrier the macrodomains formed on quartz thin films, which are described in his paper, should be visible by the eye and optical microscopy.

The samples made with DFP 3 (two pot synthesis method) did not yield any visible macrodomains by optical microscopy. AFM images, shown in figure 17, confirmed the amorphous nature of the silica film.

The samples made with DFP 4 (one pot synthesis method) did yield spots that were visible to the eye and under an optical microscope and appear to be macrodomains. AFM images of these spots, shown in figure 18, show features which look very similar to

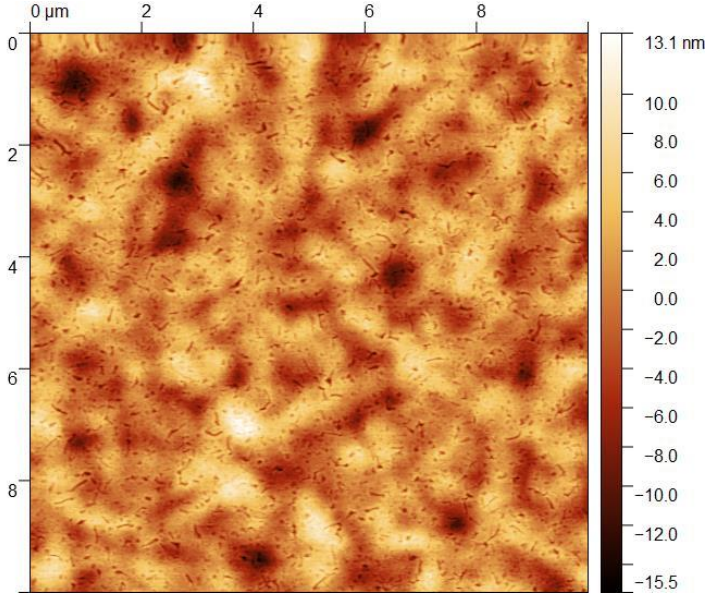

Figure 17 10x10µm AFM image of amorphous silica film produced by DFP 3

AFM images of the macrodomains reported by Carretero-Genevrier.[5] The macrodomains appear to have lines going through them in the same direction which is a sign of a preferred orientation. There seem to pores in the film which are roughly 5 nm in diameter.

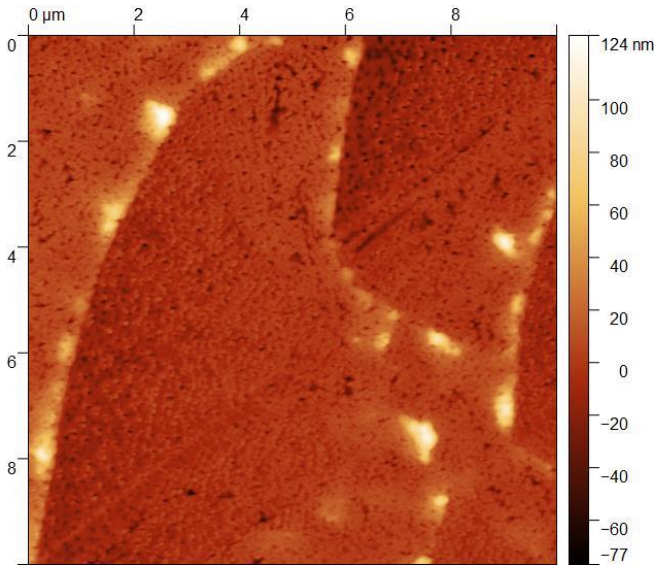

Figure 18 10x10 µm AFM image of macrodomains found on films produced by DFP 4

2theta/omega scans were performed on one of each samples to identify which crystal phases had formed. In the case of all the measurements no peaks were seen except for a multiple diffraction peak of the Si substrate at 33 degrees. There were roughly 30 spots or centers for macrodomains present across the surface. The sample was far from being homogenous. This is probably not enough to produce a signal using XRD. Reflectivity measurements were also not conclusive on the samples. No fringes were seen in these measurements so the thickness of the films is unknown.

Water droplets also formed on one of the films during the evaporation step of dip coating. This could be an indication that the RH was too high during dip coating because the concentration of the salt was not in the range to significantly draw water from the atmosphere.

A batch of samples was made where the effect of the thickness of the amorphous silica matrix on the degree of crystallization was examined. Samples were dipped either twice, three times or four times in the TEOS solution with calcination steps in between every dip coating cycle. During dip coating the vial containing the TEOS solution was placed in a beaker filled with $CaCl_2$ drying agent. This ensured that the RH was as low as possible. However the RH around the sample could not be measured. The effect of thickness on the degree of crystallinity was negligible. The samples showed the same coverage of the macrodomains as singly dipped films. The films dipped at lower RH did show an increase in the coverage of macrodomains visible after annealing compared to films made without $CaCl_2$ drying the atmosphere during dip coating. However the increase in coverage of the macrodomains was not enough to produce a signal in the XRD.

3.4 DENSE FILM PROCEDURE 5

2 films were made using DFP 5, which is the most recent and most complete version of the procedure described by Carretero-Genevrier. The procedure described in that article uses CTAB as a surfactant which leads to the formation of macropores. To make a mesoporous

amorphous silica film non-ionic surfactant Brij-C10 is used in this procedure instead. Dip coating was performed at 46% RH.

After annealing both films had around 30-40 spots or macrodomains with a diameter of roughly 100 micron, which are visible by optical microscopy, around the center of the substrate. The degree of crystallinity of the film is therefore assumed to be low.

No AFM images were made of the produced films.

2theta/omega scans were not performed on the samples due to a lack of homogenous coverage by the macrodomains.

3.5 DENSE FILM PRCOEDURE 6

Two samples were dip coated in the solution containing the TEOS and titanium tetrabutoxide and were subsequently dip coated in a solution containing either 1 M $SrCl_2$ or $LiNO_3$. One sample was only dip coated in the solution containing the TEOS and titanium tetrabutoxide. The samples were dip coated at 47% RH.

The sample dip coated only in the TEOS solution showed no signs of macrodomains on the surface of the film after annealing. Therefore it can be assumed that the bulk of the film is amorphous.

The samples dip coated in the TEOS solution and additional salt were almost completely opaque after annealing. The sample dipped in $SrCl_2$ showed marks left by recrystallized $SrCl_2$ crystals which disturb the opaque appearance of the film. The previously found macrodomains do not appear in these films.

EDS elemental mapping of the surface has to be performed to see if the Ti actually is homogenously spread through the amorphous silica matrix.

2theta/omega scans were not performed on the samples and should be performed in the future.

3.6 DENSE FILM PROCEDURE 7

Three films were made with by dipping the oxidized silicon substrates with a native oxide layer on top in a solution containing either ~2-3 M $SrCl_2$, 5 M LiCl or 5 M NaCl. After annealing fully homogenous opaque samples obtained. The sample dipped in $SrCl_2$ showed again the

marks left behind by needle shaped recrystallized $SrCl_2$. 2theta/omega scans were performed on the samples to identify which crystal phases had formed. These can be seen in figures. It was found that peaks of multiple silica polymorphs could be identified. In all cases

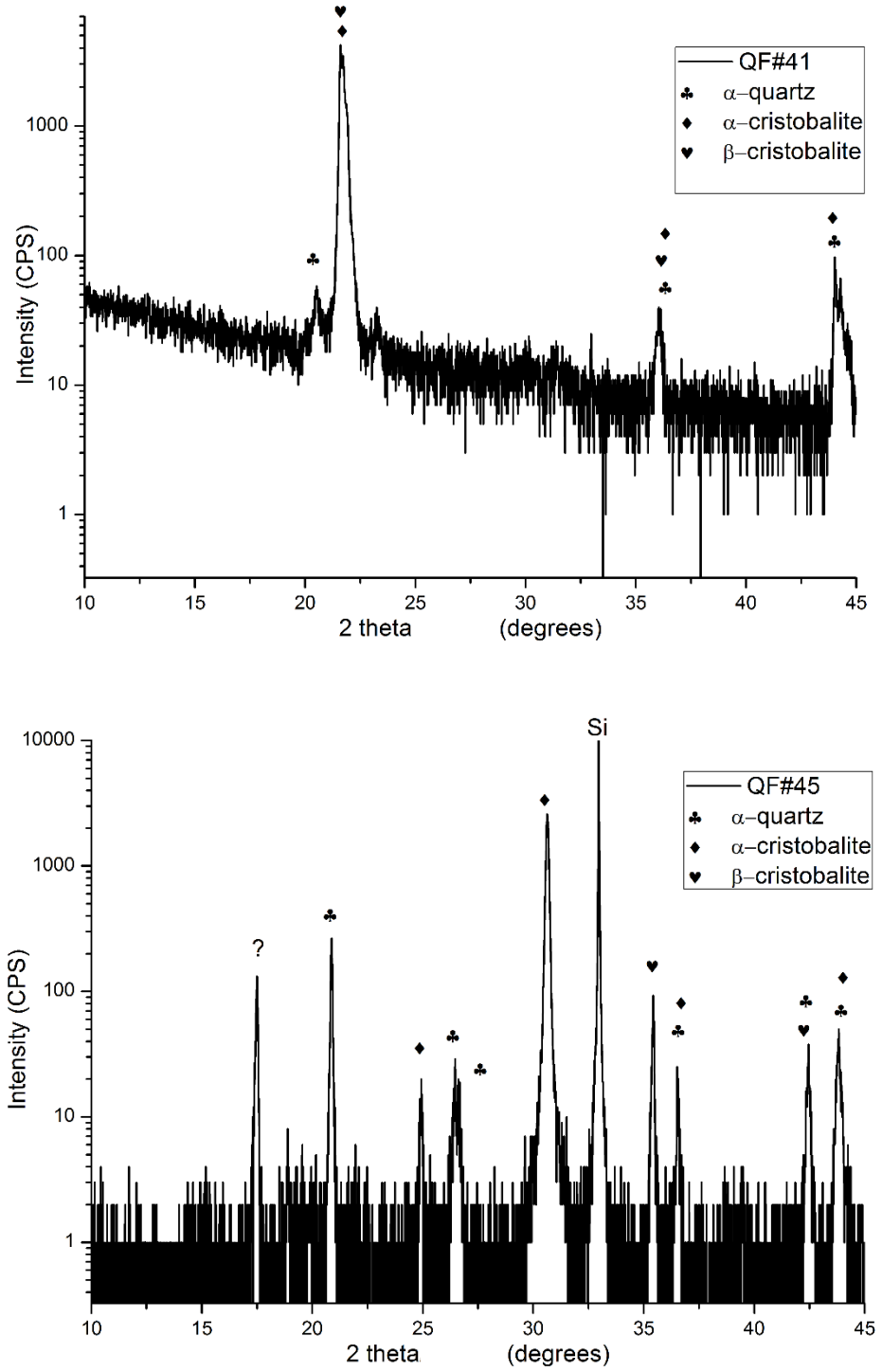

Figure 19 2 theta/omega in degrees plotted against the intensity in CPS. QF#41 was dipped in NaCl and QF#45 was dipped in $SrCl_2$.

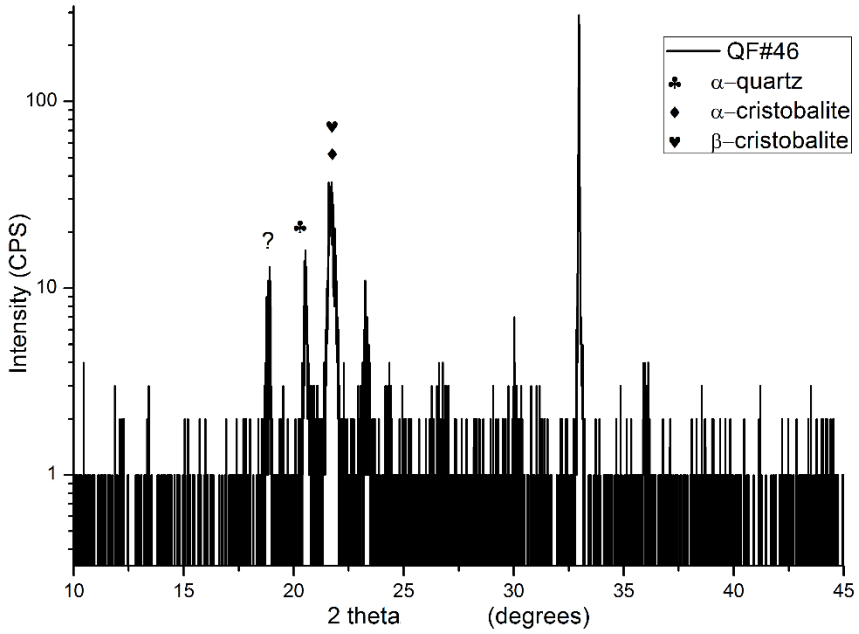

Figure 20 2 theta/omega in degrees plotted against the intensity in CPS. QF#46 was dipped in LiCl

the 100 peak of α-quartz was identified. In all cases also peaks were found that can be attributed to either α-cristobalite, β-cristobalite or α-quartz which makes analysis of the data quite difficult. The 2 theta/omega scans are shown in figures 19 and 20.

The literature reports only that cristobalite phases were found when exposing silica glass or the native oxide found on silicon to NaCl and annealing at 1100˚C.[16,17] According to this paper, the cooling rate has a significant influence on which cristobalite phase is found.[16] Cooling at 20˚C/min led to the formation of α-cristobalite while rapidly cooling at 600˚C/min led to the formation of β-cristobalite. The cooling rate is not known in this experiment but can be assumed to be slower than 20˚C/min. It makes thermodynamical sense that significantly slowing down the cooling rate of the samples could lead to the formation of the phase which is lowest in energy, namely α-quartz. That could explain why a mixture of these phases is seen on these samples.

Different salts showed different peaks in the diffraction pattern. This means that the salt choice has an effect on the orientation of the crystals with respect to the Si substrate or influences the degree of orientation of the crystals. A peak at around 15 degrees that belongs to an unknown phase was found on the films made with either $SrCl_2$ or LiCl.

A rocking curve was made of the peak at 21.8 degrees that corresponds to either α- or β-cristobalite. This is shown in figure 21. Figure 21 shows that the FWHM of the peak is 5.7˚. This means that the cristobalite phase is rather well oriented out-of-plane. This does not reveal any information about the in-pane orientations of the cristobalite phase.

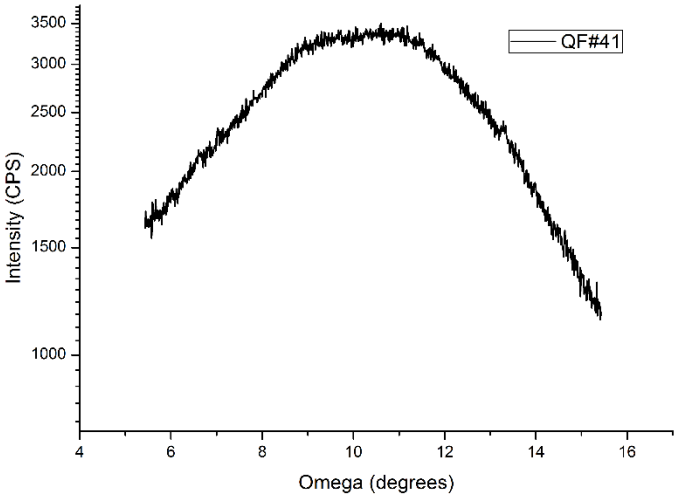

Figure 21 Rocking curve of the peak found at 2ϑ=21.8 belonging to a cristobalite phase. The FWHM is 5.7˚.

Pole figures were made of the sample that was dipped in NaCl. These are shown in figure 22.
The pole figure taken at 2theta=21.8˚ corresponds to the α- or β-cristobalite peak found in the 2th/omega scan. This pole figure shows that the highest intensity is found in the middle of the pole figure at omega=0 degrees. The pole figure shows that the spread of omega values at which this plane diffracts is roughly 10 degrees. It can be concluded that the cristobalite phase is rather well oriented.

α-cristobalite has a non-centrosymmetric crystal structure while β-cristobalite has a cubic centrosymmetric crystal structure. This means that α-cristobalite should be capable of showing piezoelectric behavior.[23] However there is little known about the piezoelectric properties of α-cristobalite.

Figure 22 also shows the pole figure taken at 2theta=20.63˚ which corresponds to the (100) plane of α-quartz. The pole figure shows noisy data with weak maximum intensities. Therefore no strong conclusions can be made from this data. However the data does indicate that there is some degree of orientation of the α-quartz phase. The most intense reflections can be seen between phi=45-135˚ and phi=225-315˚ and omega=0-20˚. This indicates that the α-quartz crystals could be twinned and tilted from omega=0 with a spread of roughly 20 degrees.

Rocking curve measurements were performed on the (102) peak of α-cristobalite found in the sample dipped in $SrCl_2$ and the (101)/(111) peak of α-cristobalite or β-cristobalite found in the sample dipped in LiCl . The measurements indicated that these crystals were not oriented. However, the alignment in these measurements was poor so better quality measurements have to be performed to accurately determine the degree of orientation of the crystals found in these samples.

The thickness of these samples could not be determined by X-ray reflectivity.
.

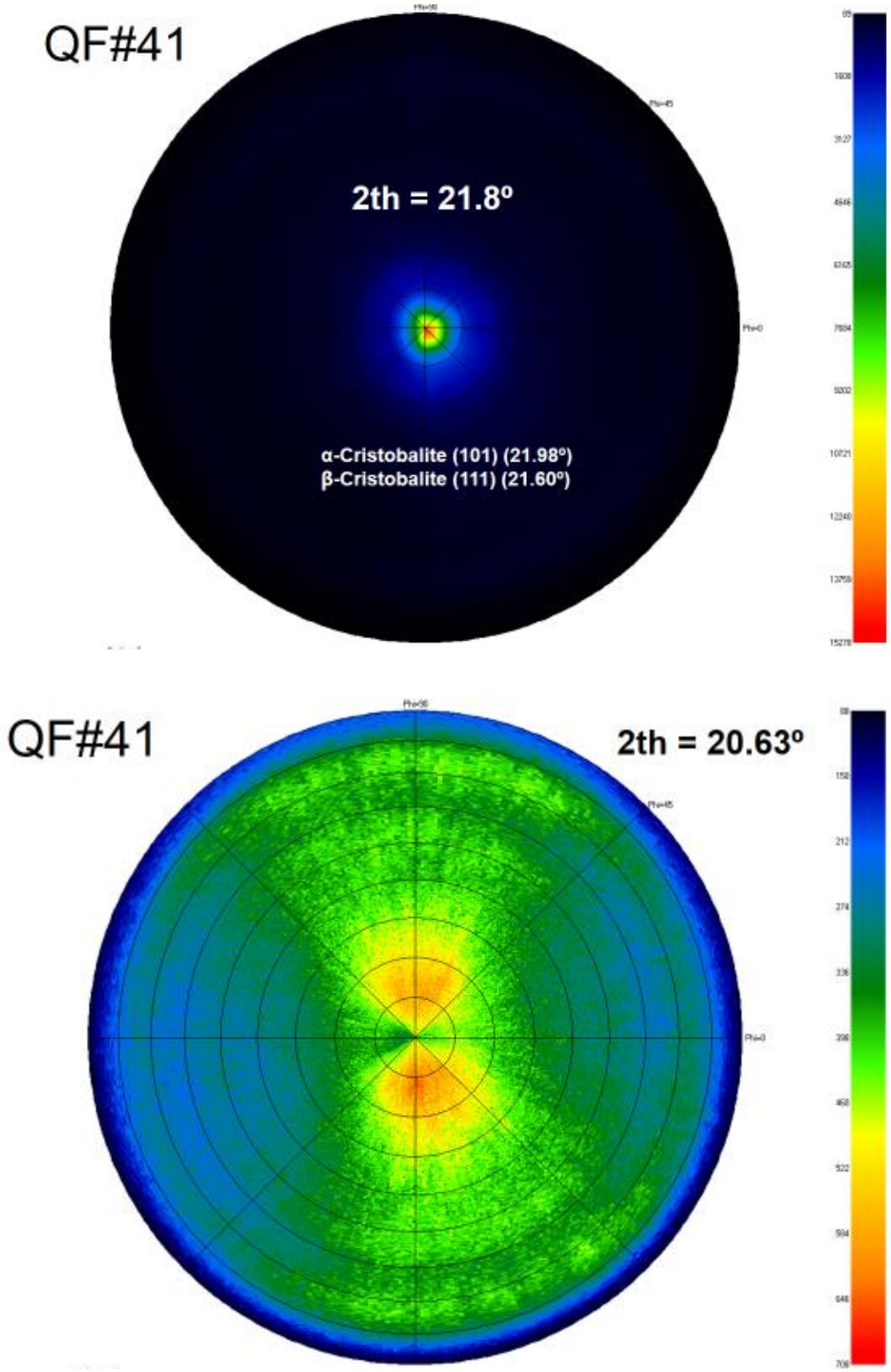

Figure 22 Pole figures taken at two different 2ϑ values showing the highly oriented nature of the cristobalite phase and the less oriented nature of the α-quartz phase

4. CONCLUSION

In this project attempts were made to synthesize epitaxial oriented α-quartz thin films using chemical solution deposition techniques. Experiments performed trying to reproduce results achieved by Carretero-Genevrier et al, resulted in highly inhomogenous thin films which were mostly amorphous silica.

It was found that the one pot synthesis methods, originally meant for producing macroporous films, produced thin films that showed more of the characteristics expected from α-quartz films than the two pot synthesis methods which only produced highly amorphous films. Films made with DFP 2 (one pot synthesis) contained oriented crystallites of an unknown crystal phase visible by AFM but lacked the macrodomains described by Carretero-Genevrier which should be visible by optical microscopy. These films were also unexpectedly macroporous which should not occur when using non-ionic surfactants. The low pH of the reaction mixture likely causes the protonation of the surfactant used, causing the surfactant to become cationic.

Films made with DFP 1 and 3, which are two pot synthesis methods, only yielded completely amorphous films except for when a droplet of salt solution was left on the surface during annealing which led to the formation of unknown crystal phases in the vicinity of the droplet. Films made with DFP 4 (one pot synthesis method) contained presumably macrodomains which were visible by eye and by optical microscopy. AFM images of the macrodomains were very similar to those shown in the literature. The coverage of the macrodomains on the films was not enough to produce a signal by XRD.

Films made with DFP 5 were almost identical to films made with DFP 4. The addition of more HCl and the use of bigger slabs of Si (100) did not produce significant changes.
The procedures based on the work of Carretero-Genevrier et al, did not produce homogenously crystallized films presumably due to the inhomogenous distribution of the metal cation catalysts throughout the amorphous silica matrix. The relative humidity at which the dip coating is performed could be the reason for this phenomenon. Dip coating the silicon substrates to produce dense quartz films should be performed between 40-55% RH and even when they were performed at 46% RH fully crystallized films did not form and even the formation of water droplets on the surface of the films during the evaporation step of dip coating was seen. Water on the surface of the films could prevent the deposition of the metal cations in the mesopores and cause them to aggregate on the surface. This indicates that dip coating should be performed at even lower RH.

Films made with DFP 6 showed that additional salt is needed for the formation of some phase on the surface of the substrate, the titanium tetrabutoxide is not enough to induce

crystallization. However the phases that formed on the films dipped in additional salt solution are still unknown due to the lack of XRD measurements.

The simple DFP 7 produced the only films on which crystal phases formed, which could be identified using XRD. The films all appeared to contain a mixture of α-quartz, α-cristobalite and β-cristobalite. The different salt solutions used for dip coating the silicon substrate produced three different XRD spectra. The choice of salt appears to have an influence on the degree of orientation of the crystallites as well as on which orientation it prefers. Rocking curve and pole figure measurements were performed on the sample that was dipped in 5 M NaCl (QF#41) that showed that the (101)/(111) peak of either α- or β-cristobalite was highly oriented. Pole figure measurements on the (100) peak of α-quartz indicate that the α-quartz crystals could be twinned and tilted with respect to the surface by roughly 20 degrees.

5. FUTURE RESEARCH/OPEN QUESTIONS

Future experiments should focus on controlling certain aspects of the synthesis and other characterization techniques should be used to get a better understanding of what is going on the films.

Future films that are made by following the procedures based on the work of Carretero-Genevrier et al, should perform the dip coating steps in an environment where the relative humidity can be controlled. Also the existence of mesopores in the amorphous silica matrix on the silicon substrate should be confirmed by for example SEM or other imaging techniques.

The crystal phases present on films made with DFP 6 should be identified by XRD measurements.

EBSD measurements should be performed on the samples produced by DFP 7. This would provide information on the degree of crystallinity of the films, the degree of orientation of the crystals that are present and the full 3D orientation of the crystals themselves. This would provide valuable information about the in-plane orientations of the crystallites as well. This measurement will also be more efficient than measuring pole figures on all the samples. EBSD measurements could also be useful for the inhomogenously crystallized films produced by DFP 4 and 5 to identify the degree of crystallinity of the film and could provide some information about which crystal phase is present on the surface as well.

Furthermore the synthesis of thin films using DFP 7 should be explored further by looking at the effect of the choice of salt and cooling time after annealing on the crystal phases that are formed on the substrate as well as the degree of orientation of these phases.

Then films of oriented pure α-cristobalite could be produced and their piezoelectric properties could be explored or enhanced by looking at the effect of the α- → β-cristobalite transition on the piezoelectric properties of the film.

6. ACKNOWDLEDGEMENTS

I would like to thank my daily supervisor Jordi Antoja Lleonart who was there every day to supervise my experiments, advise me on which experiments we could do next and with the interpretation of the results. Also I would like to thank prof. Beatriz Noheda for letting me work on this interesting project and for the helpful input and suggestions when discussing the progress of the project. Of course I would also like to thank Jacob Baas who helped with advice on all the technical aspects of the experiments and for advice in general.

7. REFERENCES

(1) Driscoll, K. Understanding quartz technology in early prehistoric Ireland, 2010.

(2) Curie, P.; Curie, J. *Comptes Rendus* **1880**, *91*, 383–386.

(3) Cady, W. G. *Proc. Am. Phys. Soc.* **1921**, *17*, 1–2.

(4) Carretero-Genevrier, A.; Gich, M.; Picas, L.; Gazquez, J.; Drisko, G. L.; Boissiere, C.; Grosso, D.; Rodriguez-Carvajal, J.; Sanchez, C. *Science (80-.).* **2013**, *340*, 827–831.

(5) Drisko, G. L.; Carretero-Genevrier, A.; Gich, M.; Gàzquez, J.; Ferrah, D.; Grosso, D.; Boissière, C.; Rodriguez-Carvajal, J.; Sanchez, C. *Adv. Funct. Mater.* **2014**, *24*, 5494–5502.

(6) Zhang, H.; Zhang, X. S.; Cheng, X.; Liu, Y.; Han, M.; Xue, X.; Wang, S.; Yang, F.; A S, S.; Zhang, H.; Xu, Z. *Nano Energy* **2015**, *12*, 296–304.

(7) Li, Z.; Zhu, G.; Yang, R.; Wang, A. C.; Wang, Z. L. *Adv. Mater.* **2010**, *22*, 2534–2537.

(8) Stöber, W.; Fink, A.; Bohn, E. *J. Colloid Interface Sci.* **1968**, *26*, 62–69.

(9) Takahashi, N.; Majima, J.; Nakumura, T.; Nonaka, S.; Yagi, H.; Shinriki, Y.; Tamanuki, K. *Chem. Mater.* **2003**, *15*, 2889–2891.

(10) Chen, M. S.; Santra, A. K.; Goodman, D. W. *Phys. Rev. B - Condens. Matter Mater. Phys.* **2004**, *69*, 1–7.

(11) Wu, S.-H.; Mou, C.-Y.; Lin, H.-P. *Chem. Soc. Rev.* **2013**, *42*, 3862.

(12) C. J. Brinker; G. W. Scherer. *Sol–Gel Science: The Physics and Chemistry of Sol–Gel Processing*; 1990.

(13) Israelachvili, J. . *Intermolecular and Surface Forces*, 3rd ed.; 2011.

(14) Grosso, D.; Cagnol, F.; Soler-Illia, G. J. D. A. A.; Crepaldi, E. L.; Amenitsch, H.; Brunet-Bruneau, A.; Bourgeois, A.; Sanchez, C. *Adv. Funct. Mater.* **2004**, *14*, 309–322.

(15) Carretero-Genevrier, A.; Gich, M.; Picas, L.; Gazquez, J.; Drisko, G. L.; Boissiere, C.; Grosso, D.; Rodriguez-Carvajal, J.; Sanchez, C. *Science* **2013**, *340*, 827–831.

(16) Nagasima, N.; Enari, H. *Jpn. J. Appl. Phys.* **1971**, *10*, 441–447.

(17) Horii, N.; Kamide, M.; Inouye, A.; Kuzuu, N. *J. Ceram. Soc. Japan* **2010**, *118*, 318–320.

(18) Okabayashi, M.; Miyazaki, K.; Kono, T.; Tanaka, M.; Toda, Y. *Chem. Lett.* **2005**, *34*, 58–59.

(19) Scriven, L. E. *Better Ceram. Through Chem. III* **1988**, *121*, 717–729.

(20) Speakman, S. A. *Introduction to High Resolution X-Ray Diffraction of Epitaxial Thin Films*; MIT Center for Materials Science and Engineering, Cambridge, 2012.

(21) Hansma, P. K.; Cleveland, J. P.; Radmacher, M.; Walters, D. A.; Hillner, P. E.; Bezanilla, M.; Fritz, M.; Vie, D.; Hansma, H. G.; Prater, C. B.; Massie, J.; Fukunaga, L.; Gurley, J.; Elings, V. *Appl. Phys. Lett.* **1994**, *64*, 1738–1740.

(22) Carretero-genevrier, A.; Gich, M. *J. Vis. Exp.* **2015**, 1–5.

(23) Williamson, B. J.; Pastiroff, S.; Cressey, G. *Atmos. Environ.* **2001**, *35*, 3539–3542.